

## Aberystwyth University

### *Bubble entrainment by a sphere falling through a horizontal soap foam*

Cox, Simon; Davies, Tudur

*Published in:*

EPL

*DOI:*

[10.1209/0295-5075/130/14002](https://doi.org/10.1209/0295-5075/130/14002)

*Publication date:*

2020

*Citation for published version (APA):*

Cox, S., & Davies, T. (2020). Bubble entrainment by a sphere falling through a horizontal soap foam. *EPL*, 130, [14002]. <https://doi.org/10.1209/0295-5075/130/14002>

#### **General rights**

Copyright and moral rights for the publications made accessible in the Aberystwyth Research Portal (the Institutional Repository) are retained by the authors and/or other copyright owners and it is a condition of accessing publications that users recognise and abide by the legal requirements associated with these rights.

- Users may download and print one copy of any publication from the Aberystwyth Research Portal for the purpose of private study or research.
- You may not further distribute the material or use it for any profit-making activity or commercial gain
- You may freely distribute the URL identifying the publication in the Aberystwyth Research Portal

#### **Take down policy**

If you believe that this document breaches copyright please contact us providing details, and we will remove access to the work immediately and investigate your claim.

tel: +44 1970 62 2400

email: [is@aber.ac.uk](mailto:is@aber.ac.uk)

# Bubble entrainment by a sphere falling through a horizontal soap foam

S.J. COX<sup>1</sup> and I.T. DAVIES<sup>1</sup>

<sup>1</sup> *Department of Mathematics, Aberystwyth University, Aberystwyth SY23 3BZ, UK*

PACS 47.57.Bc – Foams and emulsions

PACS 68.03.Cd – Surface tension and related phenomena

PACS 47.55.db – Drop and bubble formation

**Abstract** – Processes such as particle separation, froth flotation and explosion suppression rely on the extent to which particles are trapped by foam films. We simulate the quasi-static motion of a spherical particle through a stable, horizontal soap film. The soap film subtends a fixed contact angle, in the range  $10 - 135^\circ$ , where it meets the particle. The tension and pressure forces acting on the particle are calculated in two cases: when the film is held within a vertical cylinder, trapping a bubble but otherwise free to move vertically, and when the outer rim of the film is held in a fixed circular wire frame. Film deformation is greater in the second case, and the duration of the interaction therefore increases, increasing the contact time between particle and film. As the soap film returns towards its equilibrium shape following the passage of the particle a small bubble is trapped for contact angles below a threshold value of  $90^\circ$ . We quantify how the size of this bubble increases when the particle is larger and when the contact angle is smaller.

**Introduction.** – Aqueous foams interact with particles in a number of important situations [1, 2]; at high particle density the particles can even replace surfactant and stabilise the foam [3]. At the other extreme, foam films can be used to separate individual particles based on their size [4]. In between, processes such as froth flotation and explosion suppression [2, 5] rely on the extent to which particles are trapped by foam films. Once in the film, particles may rotate and, depending on parameters such as the contact angle, may cause rupture [6].

Le Goff et al. [7] found that small millimetric-sized particles falling on to a soap film at speeds of about 1 m/s do not break the film. That is, after the particle has passed through the soap film the film “heals” itself [8]. This arrangement of a stable soap film held horizontally while a small spherical particle falls onto it permits an investigation of the forces that the soap film exerts on the particle and the consequent changes to the particle’s velocity. The soap film can be considered to represent one repeating unit of a more extensive “bamboo” foam [9], in which successive impacts between the particle and different soap films could bring the particle to rest, representing a microscopic approach to the way in which a foam can be used in impact protection [5]. In the following, we choose the particle’s weight sufficiently large that it is never trapped by a sin-

gle soap film. Then the film is pulled into a catenoid-like shape as it is stretched by the particle, until, similar to the usual catenoid instability [10], the neck collapses and the soap film returns to its horizontal state.

We will show that the forces exerted on the particle depend strongly on the contact angle along the triple line (Plateau border) where the liquid, gas and solid particle meet. In an experiment this contact angle could be adjusted by coating the particle [11]. We allow the contact angle at which the soap film meets the spherical particle to vary: the equilibrium case is a contact angle of  $\theta_c = 90^\circ$  [12], in which the sphere is assumed to be coated with a wetting film that allows the soap film to move freely. However, experimental photographs [7, 13] show that the soap film wraps around the particle, with a contact angle far from  $90^\circ$ , before forming a catenoid-like neck. This suggests that the particle’s motion is faster than the mechanical relaxation of the foam. Here we nonetheless employ quasistatic simulations, and presume that the only effect of the dynamic nature of the experiments is to adjust the contact angle between particle and film. We consider several values of  $\theta_c$  down to  $10^\circ$ .

In experiments, the collapse of the catenoidal neck above the particle generates a small bubble [7], as for the impact of a liquid drop on a liquid surface [14, 15] and the

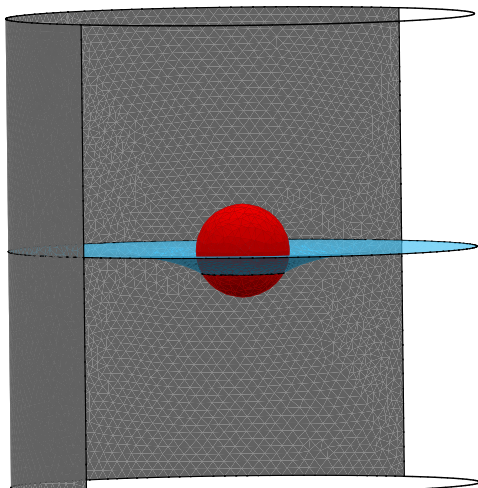


Fig. 1: A spherical particle passing through a soap film held in a cylinder. The contact angle between the particle and the film is  $30^\circ$  in this example.

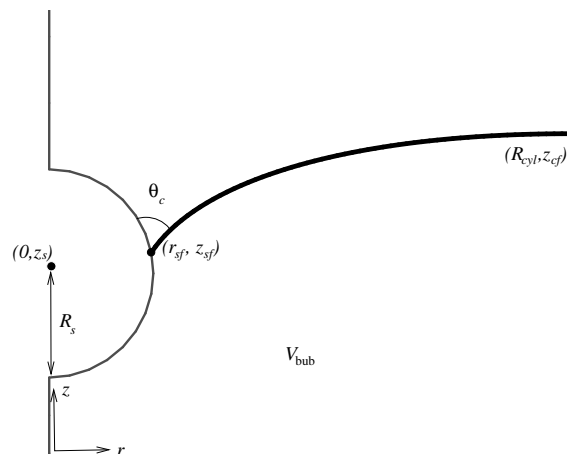


Fig. 2: The axisymmetric structure under consideration, shown in the  $(r, z)$  plane. In case 1 there is a bubble of fixed volume  $V_{\text{bub}}$  and the vertex at position  $(R_{\text{cyl}}, z_{\text{cf}})$  is free to move, while in case 2 there is no volume constraint and the vertex is fixed.

51 collapse of an isolated soap-film catenoid [16]. This small  
 52 bubble was not seen in previous simulations with a  $90^\circ$   
 53 contact angle [9, 12]. Our new simulations make clear why  
 54 this is the case: only with a contact angle smaller than  $90^\circ$   
 55 does the film curve around the particle sufficiently before  
 56 detachment to enclose such a volume of gas.

57 The particle in our simulations, described below, is a  
 58 sphere of radius  $R_s$  and mass  $m$  grams, and hence with  
 59 density  $\rho = m/(4/3\pi R_s^3)$ ; see figure 1. It falls towards a  
 60 film with interfacial tension  $\gamma$  (so a film tension of  $2\gamma$ ).  
 61 We consider two cases:

- 62 1. the soap film is held in a cylinder of radius  $R_{\text{cyl}}$  and  
 63 height  $H = 2R_{\text{cyl}}$ . The film encloses a bubble of fixed  
 64 volume  $0.5H\pi R_{\text{cyl}}^2$ , i.e. that fills the lower half of the  
 65 cylinder. In this case both the tension in the film and  
 66 the pressure in the bubble exert a force on the sphere  
 67 once it touches the film.
- 68 2. the soap film is held by a fixed ring of radius  $R_{\text{cyl}}$ . In  
 69 this case only the tension in the film exerts a force on  
 70 the sphere.

71 The Bond Number is defined as  $Bo = \frac{1}{2}\rho g R_s^2 / \gamma$ . In the  
 72 simulations we ensure that the Bond number is just greater  
 73 than one, indicating that gravitational forces should ex-  
 74 ceed the retarding force due to surface tension. Making  
 75 the density (and hence the Bond number) smaller would  
 76 lead to the sphere being trapped by the film. **In-  
 77 creasing the particle density would mean that the quasistatic ap-  
 78 proximation that we employ would be less appropriate;  
 79 indeed, balancing capillary effects with inertial effects for  
 80 the particles that we consider below, by choosing a Weber  
 81 number of one, suggests that particle velocities should be  
 82 at most 1 m/s for this approximation to be valid.**

83 **Method.** –

*Geometry.* We use the Surface Evolver [17] to com-  
 84 pute the shape of the soap film. Since this software gives  
 85 information about static situations, we **treat the motion as**  
 86 **overdamped**, and therefore the sphere and soap film move  
 87 through a sequence of equilibrium positions determined by  
 88 the forces acting.

89 By symmetry the sphere must remain in the centre of  
 90 the film, so we perform an axisymmetric calculation in the  
 91  $(r, z)$  plane (figure 2). The film is represented by a curve  
 92 whose endpoints touch, respectively, the sphere (or the  
 93 axis of the cylinder before attachment and after detach-  
 94 ment) and the outer cylinder / ring. We discretize the  
 95 curve into short straight segments of length  $dl$  and write  
 96 the energy of the system as  
 97

$$E_{\text{film}} = 2\gamma \sum_{\text{segments}} 2\pi r dl. \quad (1)$$

We restrict segments to have lengths in the range **0.01 –**  
 98 **–0.05 $R_{\text{cyl}}$**  which balances the need for accuracy with a  
 99 short computational time.

100 To include a contact angle  $\theta_c$  we add a further term to  
 101 the energy representing a spherical cap of film with tension  
 102  $2\gamma \cos \theta_c$  that covers the lower part of the sphere. This is  
 103 based on the height  $z_{sf}$  of the film where it meets the  
 104 sphere:  
 105

$$E_{\theta_c} = 2\gamma \cos \theta_c \cdot 2\pi R_s (z_{sf} - (z_s - R_s)), \quad (2)$$

106 where  $z_s$  is the height of the centre of the sphere. This  
 107 energy is set to zero before attachment and after detach-  
 108 ment.

109 In case 1 we must also account for the volume  $V_{\text{bub}}$  of the  
 110 bubble trapped beneath the soap film. We calculate this  
 111 volume based on the shape of the film and the positions  
 112 of its endpoints. There are three terms required:

$$V_1 = \sum_{\text{segments}} \pi r^2 dz$$

$$V_2 = \begin{cases} 0 & z_{sf} < z_s - R_s \\ \pi R_s^2 (z_{sf} - z_s + \frac{2}{3} R_s) - \frac{\pi}{3} (z_{sf} - z_s)^3 & z_s - R_s \leq z_{sf} \leq z_s + R_s \\ \frac{4}{3} \pi R_s^3 & z_{sf} > z_s + R_s \end{cases} \quad (3)$$

$$V_3 = \pi R_{\text{cyl}}^2 z_{cf},$$

113 with  $V_{\text{bub}} = V_3 - V_2 - V_1$ . The first term ( $V_1$ ) is the vol-  
 114 ume of revolution about the  $z$  axis of the film between its  
 115 endpoints, and the second term ( $V_2$ ) is the volume of the  
 116 spherical cap below the the point of contact between the  
 117 film and the sphere. These are both subtracted from the  
 118 third term ( $V_3$ ), which is the total cylindrical volume en-  
 119 closed by the outer wall of the cylinder beneath the point  
 120 of contact  $z_{cf}$  between the film and the cylinder wall.

121 *Forces.* We consider two forces in addition to the  
 122 weight  $mg$  acting in the negative  $z$  direction. The ten-  
 123 sion force  $F_\gamma$  is due to the pull of the soap film around  
 124 its circular line of contact with the sphere and the pres-  
 125 sure force  $F_p$ , which is only relevant in case 1, is due to  
 126 the pressure  $p_{\text{bub}}$  in the trapped bubble which acts over  
 127 the surface of the sphere below the contact line. We are  
 128 interested only in the vertical component of these forces,  
 129 since by symmetry the other components cancel.

130 We define the angle  $\theta$  that the film subtends with the  
 131 centre of the sphere,  $\tan \theta = (z_{sf} - z_s)/r_{sf}$ , and then the  
 132  $z$ -components of the forces are

$$F_\gamma = 2\gamma \cdot 2\pi r_{sf} \cos(\theta - \theta_c) \quad (4)$$

133 and

$$F_p = \pi r_{sf}^2 p_{\text{bub}}. \quad (5)$$

134 *Motion.* We perform a quasi-static simulation in  
 135 which the position of the sphere is held fixed while the  
 136 equilibrium shape of the film is found, and then the sphere  
 137 is moved a small distance in the direction of the resultant  
 138 force. In case 1 the bubble pressure is found from the  
 139 Lagrange multiplier of the volume constraint, eq. (3).

140 We start the simulation with the sphere just above a  
 141 horizontal film, and move the sphere downwards until con-  
 142 tact is made and the inner end of the film jumps to a new  
 143 position on the sphere. Then the change in the vertical  
 144 position of the sphere is determined by the net force acting  
 145 on it:

$$\Delta z_s = \epsilon (F_\gamma + F_p - mg), \quad (6)$$

146 where the small parameter  $\epsilon$ , which we think of as the  
 147 inverse of a viscosity, is taken equal to  $1 \times 10^{-5}$  (which  
 148 we find is sufficiently small not to change the results).

149 Detachment occurs when the film nears the top of the  
 150 sphere and becomes unstable, at which point it jumps  
 151 back to being horizontal, and we then end the simulation. Note  
 152 that  $\Delta z_s$  is always negative in our simulations, since the  
 153 weight of the sphere is large enough that it always exceeds  
 154 the tension force.

155 **Results.** – The simulations are performed in cgs  
 156 units, with  $R_{\text{cyl}} = 1\text{cm}$  and interfacial tension  $\gamma =$

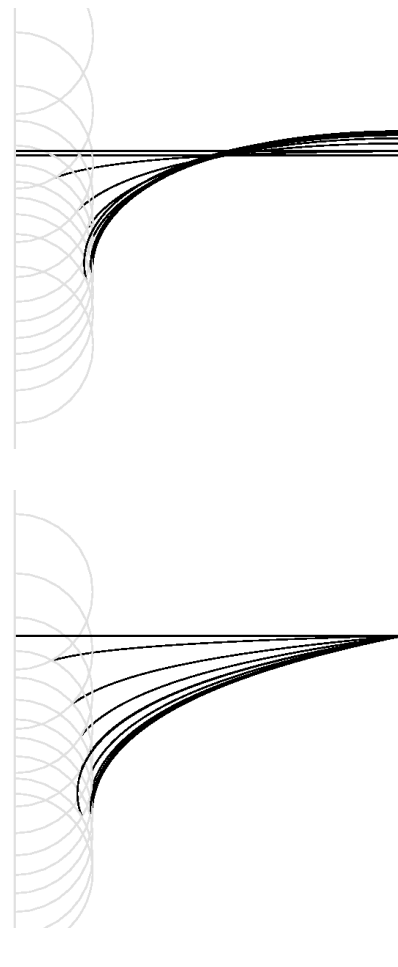
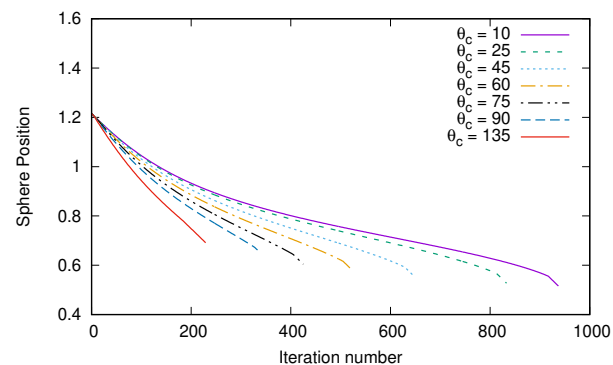


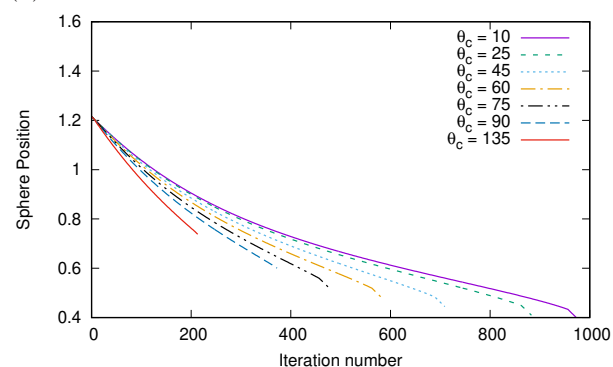
Fig. 3: Film shapes recorded as the sphere descends, with contact angle  $\theta_c = 10^\circ$ , shown every 100 iterations. (a) Case 1, where a wetting film on the outer cylinder wall allows the film to slip there and hence meet the wall at  $90^\circ$ . (b) Case 2, where the film is fixed at the outer cylinder wall. In each case, the film exhibits the greatest curvature just before detachment, and in the last sphere position shown the film has detached and returns to being horizontal.

157 30mN/m. We first consider a sphere of radius  $R_s =$   
 158  $0.2R_{\text{cyl}}$  and mass  $m = 0.1$  grams. Then the particle den-  
 159 sity is  $\rho \approx 3\text{g/cm}^3$  and the Bond number is  $Bo \approx 2$ . An  
 160 example of the shape of the film at different times is shown  
 161 in figure 3. See the supplementary material for videos of  
 162 the motion.

163 *Sphere position, soap film area, and point of contact.*  
 164 The vertical position of the centre of the sphere is shown  
 165 in figure 4. Following attachment we observe a shallower  
 166 curve for smaller contact angles, indicating that the forces  
 167 retard the motion of the sphere to a greater extent when  
 168 the contact angle is small. When the contact angle is  
 169 larger, for example with  $\theta_c$  greater than about  $45^\circ$ , the  
 170 sphere motion is at first accelerated, as the film pulls it  
 171 downwards. In case 1, the bubble pressure is also negative  
 172 at first (see figure 8 below), adding to this effect. For the

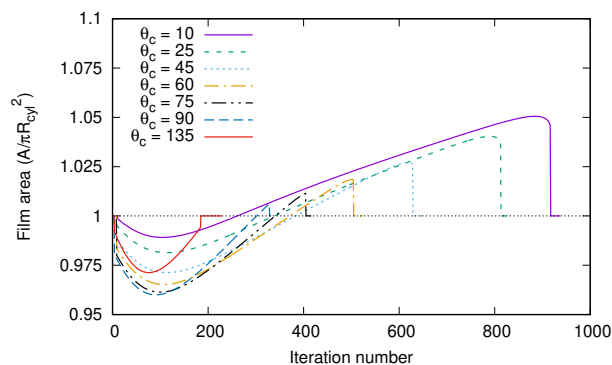


(a)

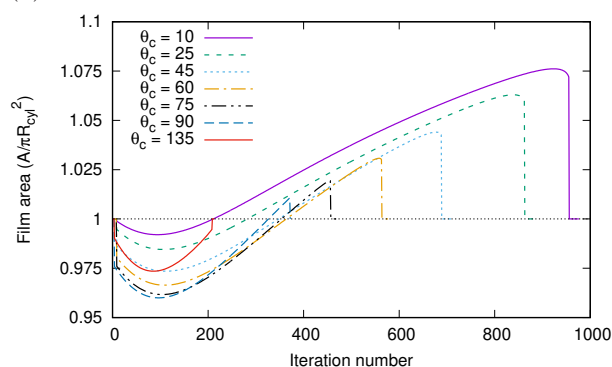


(b)

Fig. 4: The height of the centre of the sphere under the action of its weight and the forces that the foam exerts on it. The horizontal axis corresponds to time, in units of  $\epsilon$ . (a) Case 1. (b) Case 2.



(a)



(b)

Fig. 5: The area of the soap film as the sphere passes through it. (a) Case 1. (b) Case 2.

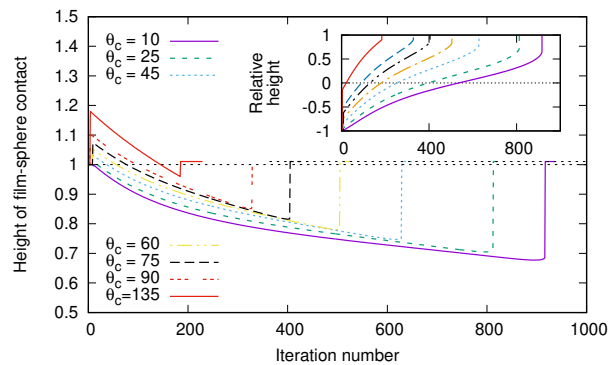
173 contact angle of  $\theta_c = 135^\circ$  this significantly reduces the  
 174 time of interaction before the film detaches from the top  
 175 of the sphere.

176 When the sphere first meets the film the film area is  
 177 reduced (figure 5) because it contains a circular hole that  
 178 is filled by the sphere. As the sphere descends further,  
 179 the film deforms in order to obey the volume constraint  
 180 (in case 1) or the fixed rim at the cylinder wall (in case  
 181 2) and to satisfy the contact angle where they meet. This  
 182 causes the film area to increase, until the film approaches  
 183 the point of detachment. For contact angles above  $90^\circ$   
 184 (for example  $\theta_c = 135^\circ$ ) the area of the film never ex-  
 185 ceeds its equilibrium value,  $A = \pi R_{\text{cyl}}^2$ , indicating that  
 186 it is not greatly deformed and that detachment occurs  
 187 quickly. Comparing case 1 to case 2, for all other contact  
 188 angles simulated, the film is slightly more deformed when  
 189 its outer rim is fixed (case 2).

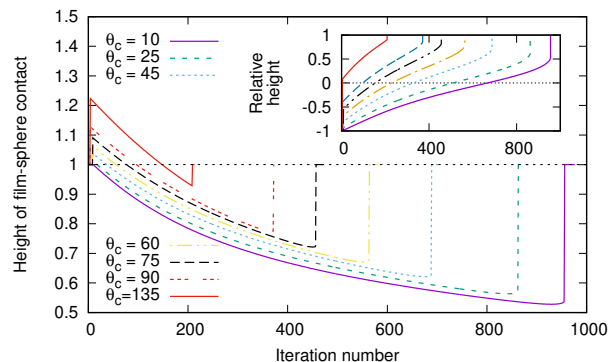
190 There is a jump in the vertical position of the circular  
 191 line of contact when the film first meets the sphere  
 192 (figure 6). The contact line rises to a new position to sat-  
 193 isfy the contact angle (without, in case 1, violating the  
 194 volume constraint), to a degree that increases with the  
 195 contact angle. This end of the film is then pulled down  
 196 by the sphere, more so for large contact angles, and the  
 197 decrease is monotonic.

198 Detachment occurs *before* the inner end of the soap film  
 199 reaches the top of the sphere. Instead, there is a sort of  
 200 “pre-emptive” instability [18]: the curved soap film be-  
 201 comes unstable, the line of contact jumps upwards, and a  
 202 new configuration consisting of a flat film above the sphere  
 203 is reached. This is seen, for example, in the abrupt jump  
 204 in the surface area of the film, shown in figure 5, at the  
 205 point of detachment. Fixing the outer rim of the film (case  
 206 2) leads to a greater deformation of the film (figure 5) and  
 207 hence to the film becoming unstable when the line of con-  
 208 tact is further from the top of the sphere (figure 6 insets).  
 209 In case 1, the film returns to a higher position after the  
 210 sphere has passed, because the volume enclosed beneath  
 211 the film is augmented by the volume of the sphere. In  
 212 case 2, without a volume constraint, the interaction time  
 213 (when the film and sphere are in contact) is longer for each  
 214 value of contact angle compared to case 1, and the sphere  
 215 descends further before detachment. Hence the overall ef-  
 216 fect of constraining the volume rather than the outer rim  
 217 of the film is to retard the sphere.

218 In case 1 the outer rim of the film, where it touches  
 219 the cylinder wall, behaves slightly differently (data not  
 220 shown). It at first drops suddenly, i.e. in the opposite  
 221 sense to the inner contact line, and then increases until  
 222 the inner contact line approaches the top of the sphere.  
 223 It then descends again before suddenly returning to the  
 224 same vertical position as the inner contact line when the

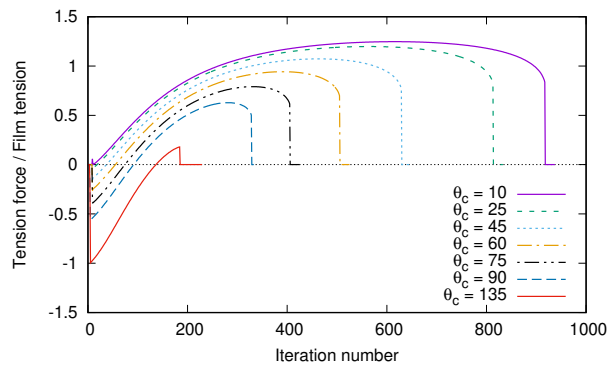


(a)

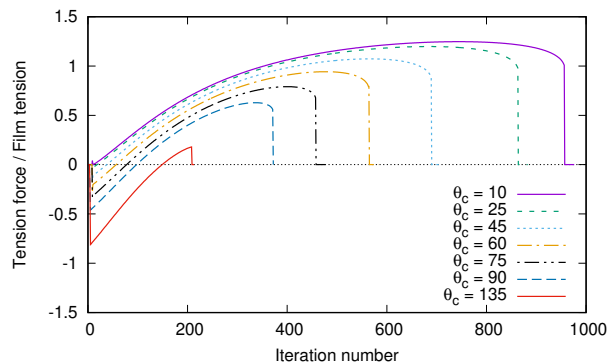


(b)

Fig. 6: The vertical position  $z_{sf}$  of the line where the film touches the sphere. The inset shows this position relative to the height of the centre of the sphere,  $(z_{sf} - z_s)/R_s$ . (a) Case 1. (b) Case 2.



(a)



(b)

Fig. 7: Tension forces exerted on the sphere, determined by the direction in which the film pulls multiplied by its tension. (a) Case 1. (b) Case 2.

225 film detaches and becomes flat.

226 *Measured forces.* We show the forces acting on the  
 227 sphere in figures 7 and 8. For large contact angles the  
 228 film pulls the sphere downwards, accelerating its motion.  
 229 The opposite occurs for small contact angles, and so the  
 230 time over which the sphere contacts the sphere is extended.  
 231 Just before the abrupt drop in force at the point of detach-  
 232 ment, there is a slight reduction in the tension force as the  
 233 perimeter of the contact line becomes small, ameliorating  
 234 the pull from the film.

235 In case 1, the pressure in the bubble can be either posi-  
 236 tive or negative, depending on the curvature of the film.  
 237 The pressure force on the sphere is determined by this  
 238 pressure multiplied by the vertically-projected area of the  
 239 sphere over which the bubble touches the sphere, eq. (5).  
 240 The pressure force is much smaller in magnitude than the  
 241 tension force. For the contact angle of  $135^\circ$  the bubble  
 242 pressure is large and negative for much of the passage of  
 243 the sphere, because of the curvature induced by the con-  
 244 tact angle, so in this case the pressure force “sucks” the  
 245 sphere downwards and detachment occurs earlier than in  
 246 case 2.

247 For smaller contact angles, for example  $\theta_c = 10^\circ$ , the  
 248 pressure is always positive, opposing the downward motion  
 249 of the sphere. Yet it is still the case that detachment

250 occurs sooner in case 1, even though for a given contact  
 251 position the tension force is similar in both cases. Further,  
 252 the film becomes unstable at a lower position in case 2.  
 253 The resolution of this apparent paradox is that when the  
 254 contact line is at a certain position on the sphere, the  
 255 sphere is at a different height in the two cases, because  
 256 of the need to satisfy the different constraints and for the  
 257 film to meet the sphere at the same contact angle. In  
 258 particular, before the contact line passes the equator of  
 259 the sphere ( $z_{sf} < z_s$ ), it moves around the sphere more  
 260 slowly in case 2, while above the equator it moves more  
 261 quickly (but over a shorter distance).

262 *Bubble entrainment.* Although our quasistatic simu-  
 263 lations do not resolve the rapid film motion during detach-  
 264 ment, we can gain an idea of the size of the small bubble  
 265 that is trapped [7] by examining the shape of the soap film  
 266 immediately before detachment, as shown in figure 9. **Our  
 267 idea is that the inner part of the film rotates rapidly to-  
 268 wards the vertical axis of the cylinder during detachment,  
 269 and that the shaded region doesn’t change its shape dur-  
 270 ing this motion. Then, when the film touches the axis  
 271 part-way along its length, this volume of gas is trapped.**  
 272 We calculate the area of the region in the  $(r, z)$  plane that  
 273 is shaded in the figure, between the soap film and a ra-  
 274 dial line through the point of the soap film closest to the  
 275 vertical axis. This is likely to be an underestimate as the

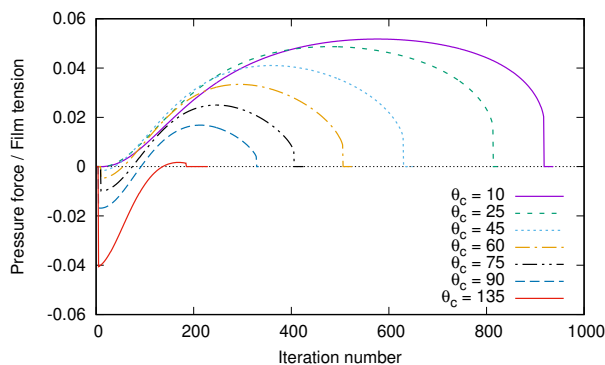


Fig. 8: Pressure forces exerted on the sphere in Case 1.

276 curvature of the film around the catenoidal neck is likely  
277 to increase during detachment.

278 Figure 9 shows that for small contact angles the bubble  
279 size can reach almost  $0.01\text{cm}^3$ . The limit in which the  
280 contact angle tends to zero appears to give a well-defined  
281 value for the maximum size of this small satellite bubble.  
282 For contact angles of  $90^\circ$  and above there is no bubble  
283 because the point on the soap film nearest to the vertical  
284 axis is where the film touches the particle.

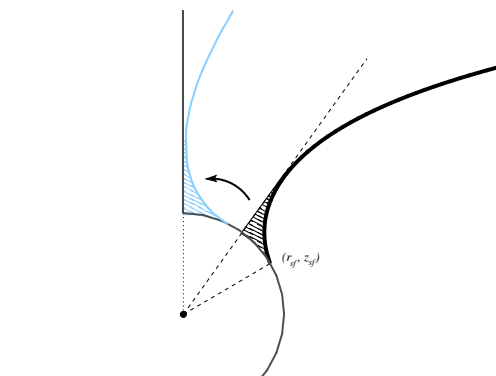
285 There is a small effect of the choice of boundary con-  
286 ditions: in case 2, without a pressure force, the bubble  
287 is about 30% larger for  $\theta = 10^\circ$  (although this difference  
288 decreases as the contact angle increases). This is because,  
289 as noted above, in case 2 the instability that causes the  
290 film to detach occurs earlier, when the line of contact is  
291 closer to the equator of the sphere.

292 In case 1 with a fixed contact angle of  $10^\circ$  we varied the  
293 size of the spherical particle and again estimated the size  
294 of the trapped bubble. For a sphere of a given radius, we  
295 must choose between a fixed particle mass (weight) or a  
296 fixed particle density.

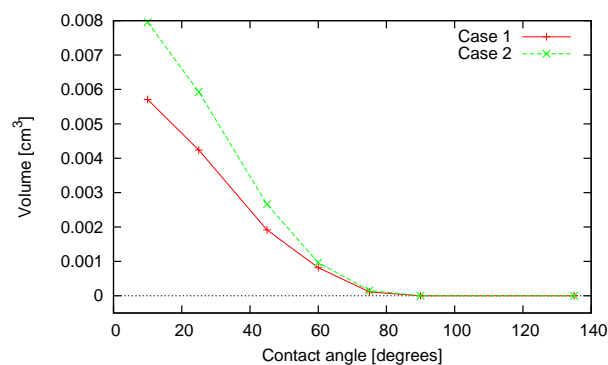
297 In the former case, the tension force opposing the de-  
298 scent of the particle increases with particle radius, but  
299 since the sphere does not increase in weight, it is brought  
300 to rest by the soap film once the particle exceeds a critical  
301 radius. The maximum vertical tension force that the soap  
302 film could exert on the sphere to counteract its weight oc-  
303 curs when the film meets the sphere on its equator and  
304 pulls vertically upwards; then the film tension multiplied  
305 by the sphere circumference is  $4\pi\gamma R_s$ . So the critical  
306 radius is  $R_{s(m)} \approx mg/(4\pi\gamma)$ . With  $m = 0.12\text{g}$  this is  
307  $R_{s(m)} \approx 0.31\text{cm}$ .

308 In the latter case, only when the particle falls below a  
309 critical radius is it brought to rest by the soap film,  $R_{s(\rho)} \approx$   
310  $\sqrt{3\gamma/(\rho g)}$ . With  $\rho = 6\text{g/cm}^3$  this is  $R_{s(\rho)} \approx 0.12\text{cm}$ .

311 Figure 10 shows that the size of the bubble that is  
312 trapped is the same in both cases. So it is determined  
313 by the shape of the soap film only, which in turn arises  
314 from the film meeting the sphere, of whatever radius, at  
315 the given contact angle. Therefore the size of the trapped  
316 bubble increases with sphere size, since the film is more  
317 greatly deformed when the sphere is larger. This also val-



(a)



(b)

Fig. 9: (a) Close to the contact line between the soap film  
and the sphere, at the last iteration before detachment (dark  
shading), we calculate the shaded volume to estimate the vol-  
ume of the small bubble that would be left behind if this region  
moved uniformly toward the axis (light shading). (b) The bub-  
ble volume depends strongly on the contact angle, depends only  
weakly on whether we consider case 1 or case 2, and vanishes  
for contact angles greater than  $90^\circ$ .

indates that our choice of  $\epsilon$  is sufficiently small that the  
numerical method works even if, for heavy particles, the  
sphere descends quickly.

There is also a small dependence of the size of the  
trapped bubble on the cylinder size. As the cylinder be-  
comes larger, the sphere descends further before detach-  
ment, and so greater film deformation is possible. In ad-  
dition, the pressure force is reduced in a larger cylinder,  
so the result should be closer to case 2. Thus, the trapped  
bubble is slightly larger if the cylinder radius is larger.

To validate our predictions, we compare with the image  
in Figure 1 of [7], which shows a sphere of radius  $0.16\text{cm}$   
falling through a soap film trapping a bubble. (The cylin-  
der radius and sphere mass are not recorded.) The bub-  
ble is trapped against the upper part of the sphere, but  
appears to be roughly hemispherical with radius  $0.08\text{cm}$ ,  
and hence a volume of  $0.001\text{cm}^3$ . The data point, shown  
in figure 10, lies close to our prediction.

**Conclusions.** — We have explained the effect of con-  
tact angle on the forces that act on a spherical particle  
passing through a soap film. The duration of the interac-

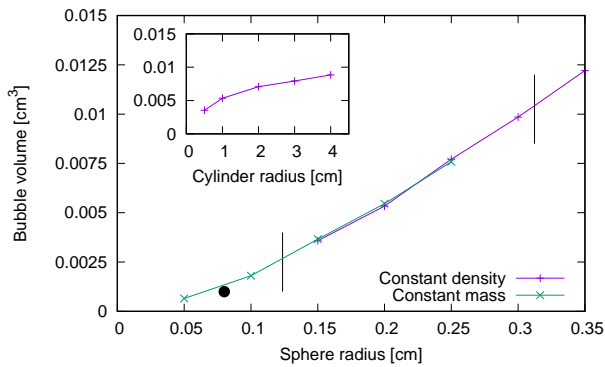


Fig. 10: With contact angle  $\theta_c = 10^\circ$  in case 1, the volume of the bubble that is trapped by the film increases with the size of the particle and (inset) depends weakly on the size of the cylinder containing the soap film. **The solid circle is experimental data [7]. With fixed mass only spheres with radius up to  $R_{s(m)}$  pass through the film; with constant density only spheres with radius larger than  $R_{s(\rho)}$  pass through the film; these bounds are indicated by the vertical lines. The size of the trapped bubble is the same in both cases, indicating that it is determined by the geometry of the soap film.**

tion is determined by the contact angle and also the way in which the film is deformed; for example, with low contact angles the particle moves more slowly, and stays in contact with the soap film for longer. Further, the interaction depends upon the details of the experiment: greater deformation is induced by holding the film in a fixed circular wire frame than in a cylindrical tube, where it traps a bubble but where the outer circumference of the film is not fixed, such as in a soap-film meter [13]. In the latter case there is an additional force on the particle due to the pressure in the bubble, but this is negligible in determining the dynamics of the system.

Analysing the shape of the soap film just before detachment allows us to predict the size of the small bubble that is formed when a particle passes through a film. The entrainment of this air and the formation of interface could play a role in determining the efficacy of using foams for the suppression of explosions. We find that the bubble increases in size as the particle gets larger, and can exceed  $10\text{mm}^3$ .

Extending our predictions to more general cases, such as oblique impact and non-spherical particles [6, 12], will require more computationally-intensive three-dimensional simulations.

\* \* \*

The late J.F. Davidson inspired us to work on this problem. We are also grateful to C. Raufaste for useful discussions, and to K. Brakke for provision and support of the Surface Evolver software. SJC acknowledges financial support from the UK Engineering and Physical Sciences Research Council (EP/N002326/1).

## REFERENCES

- [1] D. Weaire and S. Hutzler. *The Physics of Foams*. Clarendon Press, Oxford, 1999.
- [2] I. Cantat, S. Cohen-Addad, F. Elias, F. Graner, R. Höhler, O. Pitois, F. Rouyer, and A. Saint-Jalmes. *Foams - structure and dynamics*. OUP, Oxford, 2013.
- [3] B.P. Binks and R. Murakami. Phase inversion of particle-stabilized materials from foams to dry water. *Nature Mat.*, **5**:865–869, 2006.
- [4] B.B. Stogin, L. Gockowski, H. Feldstein, H. Claire, J. Wang, and T.-S. Wong. Free-standing liquid membranes as unusual particle separators. *Science Advances*, 4:eaat3276, 2018.
- [5] M. Monloubou, M. A. Bruning, A. Saint-Jalmes, B. Dollet, and I. Cantat. Blast wave attenuation in liquid foams: role of gas and evidence of an optimal bubble size. *Soft Matter*, **12**:8015–8024, 2016.
- [6] G. Morris, S.J. Neethling, and J.J. Cilliers. Modelling the self orientation of particles in a film. *Minerals Engng.*, **33**: 87–92, 2012.
- [7] A. Le Goff, L. Courbin, H.A. Stone, and D. Quéré. Energy absorption in a bamboo foam. *Europhys. Lett.*, **84**:36001, 2008.
- [8] L. Courbin and H. A. Stone. Impact, puncturing, and the self-healing of soap films. *Physics of Fluids*, 18:091105, 2006.
- [9] I.T. Davies and S.J. Cox. Sphere motion in ordered three-dimensional foams. *J. Rheol.*, **56**:473–483, 2012.
- [10] S.A. Cryer and P.H. Steen. Collapse of the soap-film bridge: quasistatic description. *J. Coll. Interf. Sci.*, **154**: 276–288, 1992.
- [11] M. A. C. Teixeira, S. Arscott, S. J. Cox, and P. I. C. Teixeira. When is a surface foam-phobic or foam-philic? *Soft Matter*, 14(26):5369–5382, 2018.
- [12] I.T. Davies. Simulating the interaction between a descending super-quadric solid object and a soap film. *Proc. Roy. Soc. A*, **474**:20180533, 2018.
- [13] C.-H. Chen, A. Perera, P. Jackson, B. Hallmark, and J.F. Davidson. The distortion of a horizontal soap film due to the impact of a falling sphere. *Chem. Eng. Sci.*, 206:305–314, 2019.
- [14] H. N. Oguz and A. Prosperetti. Bubble entrainment by the impact of drops on liquid surfaces. *J. Fluid Mech.*, 219: 143179, 1990.
- [15] S. T. Thoroddsen, K. Takehara, T. G. Etoh, and Y. Hatsuki. Puncturing a drop using surfactants. *J. Fluid Mech.*, 530:295304, 2005.
- [16] N.D. Robinson and P.H. Steen. Observations of singularity formation during the capillary collapse and bubble pinch-off of a soap film bridge. *J. Coll. Interf. Sci.*, **241**:448–458, 2001.
- [17] K. Brakke. The Surface Evolver. *Exp. Math.*, **1**:141–165, 1992.
- [18] S. Hutzler, D. Weaire, S.J. Cox, A. Van der Net, and E. Janiaud. Pre-empting Plateau: the nature of topological transitions in foam. *Europhys. Lett.*, **77**:28002, 2007.